Bioorganic Chemistry 82 (2019) 129–138

Contents lists available at ScienceDirect

Bioorganic Chemistry

journal homepage: www.elsevier.com/locate/bioorg

Design and synthesis of novel potent anticoagulant and anti-tyrosinase pyranopyrimidines and pyranotriazolopyrimidines: Insights from molecular docking and SAR analysis

Meriem Debbabi[a], Vijaykumar D. Nimbarte[b], Samia Chekir[a], Sarra Chortani[a], Anis Romdhane[a], Hichem Ben jannet[a,*]

[a] Laboratory of Heterocyclic Chemistry, Natural Products and Reactivity (LR11ES39), Team: Medicinal Chemistry and Natural Products, Faculty of Science of Monastir, University of Monastir, Avenue of Environment, 5019 Monastir, Tunisia
[b] Laboratory of Chemistry, URCOM, EA 3221, INC3M CNRS-F3038, UFR of Science and Technology, University of Le Havre, BP 1123, 25 rue Philipe Lebon, 76063 Le Havre Cedex, France

ARTICLE INFO

Keywords:
Pyranopyrimidines
Pyranotriazolopyrimidines
Anticoagulant
Anti-tyrosinase
Molecular docking
SAR

ABSTRACT

Pyrimidine-fused compounds are of great interest for the discovery of potent bioactive agents. This study describes the synthesis of novel pyranopyrimidines **3a-f** and pyranotriazolopyrimidines **4a-d** derivatives *via* the cyclocondensation reaction of α-functionalized iminoether **2**, which was obtained from 2-amino-3-cyanopyrane **1**, with a series of primary aromatic amines and hydrazides, respectively. Structures of all synthesized compounds were established on the basis of spectroscopic methods including ^{1}H NMR, ^{13}C NMR and ES-HRMS. They were finally tested for their anticoagulant and anti-tyrosinase activities. Significant results have been obtained and the structure-activity relationship (SAR) was discussed with the help of molecular docking analysis.

1. Introduction

Designing of novel class of bioactive heterocycles and develop efficient methods for their synthesis with predefined functionalities is a challenging task in modern organic chemistry [1,2]. Pyrimidines constitute an interesting group of heterocylic compounds many of which possess wide-spread pharmacological properties and their chemistry and bioactivities are receiving considerable attention and has been documented in several reports [3–6]. Furthermore, the multiple biological activities of these heterocyclic compounds are of increasing interest as antibacterial [7], antiviral [8] and antitumor [9]. In addition, some of them have shown anticoagulant (Fig. 1-A) [10] and anti-tyrosinase activities (Fig. 2-D) [11].

On another hand, pyrane-fused compounds have, for a long time, attracted the interests of both synthetic and biological researchers alike because of their various chemical and biological properties [12–14]. Many of them displayed a broad range of biological activities such as analgesic [15], antituberculosis [16], antiviral [17], anticoagulant (Fig. 1-B) [18] and anti-tyrosinase (Fig. 2-E) [19].

Furthermore, triazoles are a class of compounds, which occupies a special role in nature. They have attracted intense interest in recent years because of their diverse pharmacological properties like antibacterial [20], analgesic [21], anti-inflammatory [21] and particularly anticoagulant (Fig. 1-C) [22] and anti-tyrosinase agents (Fig. 2-F) [23].

In view of the above observations and as a continuation of our previous work on the synthesis of a new fused-pyrimidine scaffold [24–26], we report here the synthesis of some new condensed pyrimidine derivatives **3** and **4** (Fig. 3) bearing in their structures fragments such as pyrane, pyrimidine and triazole, commonly found in anticoagulant and anti-tyrosinase agents.

All synthesized compounds **1**, **2**, **3a-f** and **4a-d** were evaluated for their anticoagulant by measuring the aPTT and for their anti-tyrosinase potency and the structure–activity relationship (SAR) was discussed with the help of molecular docking analysis.

2. Results and discussion

2.1. Chemistry

The 2-amino22123-cyanopyrane **1** has served as a key starting material. It was prepared *via* one-pot three-component reaction [27], of arylaldhyde, malononitrile and 5,5-dimethylcyclohexane-1,3-dione. Since such system constitutes a commonly used building block for the

* Corresponding author.
E-mail address: hichem.bjannet@gmail.com (H. Ben jannet).

https://doi.org/10.1016/j.bioorg.2018.10.004
Received 2 August 2018; Received in revised form 21 September 2018; Accepted 4 October 2018
Available online 05 October 2018
0045-2068/

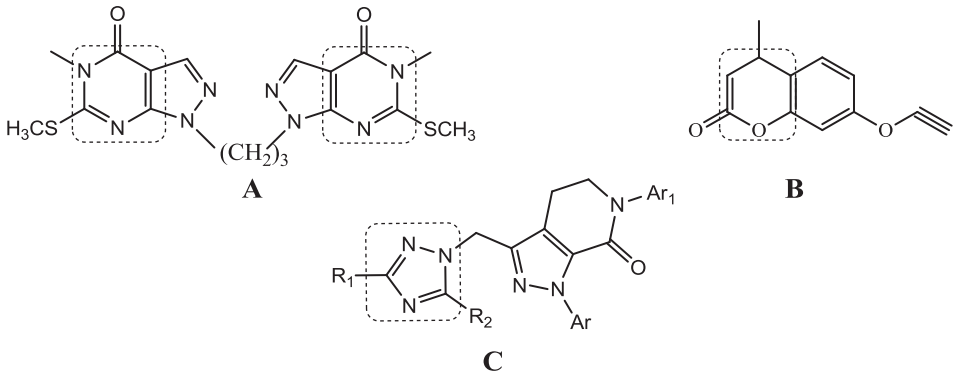

Fig. 1. Previously reported anticoagulant compounds.

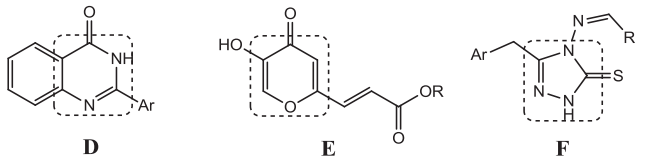

Fig. 2. Previously reported anti-tyrosinase compounds.

construction of a variety of poly-heterocycles [28,29]. For this purpose and as described in Schemes 2 And 3, our approach to the target systems **3** and **4** was firstly started by the construction of the α-functionalized iminoether **2**, *via* condensation reaction of precursor **1** with triethylorthoformate under reflux of acetic anhydride (Scheme 1) [30].

Structures of compounds **1** and **2** were established by their ^{1}H NMR and ^{13}C NMR spectra.

Then, the reflux of iminoether **2** with some primary aromatic amines in ethanol for 5 h and in the presence of a catalytic amount of acetic acid led to new the pyranopyrimidines **3** (Table 1). Plausible pathway involves two successive nucleophilic additions of the $-NH_2$ group on the imidic carbon and on the cyano function (Scheme 2).

The structures of compounds **3** have been assigned from their ^{1}H NMR, ^{13}C NMR and mass spectrometry (ES-HRMS) analytical data. In fact, the ^{1}HNMR spectra of compounds **3** showed, in addition to the new signals corresponding to the protons introduced by the intermediate **2**, the appearance of new signals due to the primary aromatic amine and the disappearance of the signals relative to the ethoxy group protons. Analysis of ^{13}C NMR spectra of the same compounds showed the appearance of a new signals relative to carbons introduced by the primary aromatic amine used, in addition to the disappearance of three signals at δ_C 13.2, 63.8 and 118.3 attributable to $\underline{C}H_3-CH_2-O$, $CH_3-\underline{C}H_2-O$ and $-CN$, respectively.

In the second part of this work, a series of new pyranopyrimidine derivatives containing the 1,2,4-triazolo moiety **4a-d** has been prepared, by cyclocondensation reaction of the precursor **2**, *via* its imidic carbon and nitrile functional group with appropriate acid hydrazides according to the procedure described by Abdel-Aziz et al. [31] (Scheme 3). This reaction was conducted in three solvents (dioxane, ethanol and toluene) and the best yields (60–85%) were obtained with dioxane (Table 2).

Plausible pathway involves two successive nucleophilic additions of $-NH_2$ group on the imidic carbon then on the cyano function followed by dehydrocyclization to give the new pyranotriazolopyrimidines **4a-d** (Scheme 3).

The formed compounds **4** were characterized by their ^{1}H NMR, ^{13}C NMR and mass spectrometry (ES-HRMS) spectral data.

Further, the ^{1}H NMR spectra of new pyranotriazolopyrimidines **4a-d** showed the disappearance of signals (triplet and quadruplet) relative to the ethoxy group of the α-functionalized iminoether **2** and the appearance of new signals, attributable to protons introduced by the appropriate hydrazide, of which chemical shifts and multiplicities are in agreement with the proposed structures.

Analysis of ^{13}C NMR spectra of compounds **4a-d** showed, in addition of the signals relative to the hydrazide moiety carbons, essentially the new signal at δ_C 152.3 relative to carbon C_2, the disappearance of two signals at δ_C 13.2 and 63.8 corresponding to the ethoxy group carbons.

The ESI-HRMS showed the correct protonated molecular ion peaks $[M+H]^+$ for all examined compounds **3** and **4**.

2.2. Biological activity

All the synthesized compounds **1**, **2**, **3a-f** and **4a-d** have been evaluated for their anticoagulant and anti–tyrosinase activities.

2.2.1. Anticoagulant activity

Anticoagulants have been introduced therapeutically for over half a century and are widely used in various fields such as surgery and cardiology. Since their introduction in therapeutics, important advances have been made, allowing a better understanding of their mechanism of action, the intimate mechanisms of thrombosis, the role of platelets and the endothelium. Thus, with the progress of methods of synthesis and the isolation from natural sources, new molecules were discovered.

Anticoagulants block the vitamin K cycle by acting on epoxide reductase and inhibiting the quinonereductase responsible for the transformation of vitamin K epoxide (KO) into vitamin K quinone, responsible for blood coagulation.

The *in vitro* anticoagulant activity of all the synthesized compounds **1**, **2**, **3a-f** and **4a-d** was evaluated by measuring the activated Partial Thromboplastin Time (aPTT) in normal human plasma. As shown in Table 3, all the synthesized compounds have displayed good anticoagulant activities expressed by the significant prolongation of aPTT in a concentration–dependent manner ranging from 53.7 to 72.8 s compared to that of the negative control (aPTT = 33.0 s).

From the results obtained, it has been found that the iminoether **2** exhibited the highest activity (aPTT = 72.8 ± 0.9 s) followed by the starting product **1** (aPTT = 68.3 ± 0.8 s) compared to the plasma as negative control (aPTT = 33.50 ± 0.05 s). The prepared pyranopyrimidines **3a-f** exhibited good anticoagulant activity with aPTT values ranging from 53.7 ± 0.9 to 63.2 ± 1.1 s. In this series, compound **3f** bearing a naphthyl group displayed the highest activity (aPTT = 63.2 ± 1.1 s) followed by **3c** with a 4–C_2H_5Ph (aPTT = 61.8 ± 1.0 s) whereas **3b** (3–CH_3Ph) was found to be the less active (aPTT = 53.7 ± 0.9 s) but remains more effective than the negative control (plasma). This difference in activity could be explained by the nature and the position of the alkyl group attached to the aromatic ring. Compound **3e** with a 4–OCH_3–Ph showed a slightly higher activity than its analogue **3d** (3-ClPh) (aPTT = 57.0 ± 1.0 and 54.8 ± 0.8 s, respectively). This finding could be due to the nature of the substituent and its own electronic effect. Indeed, the methoxy group

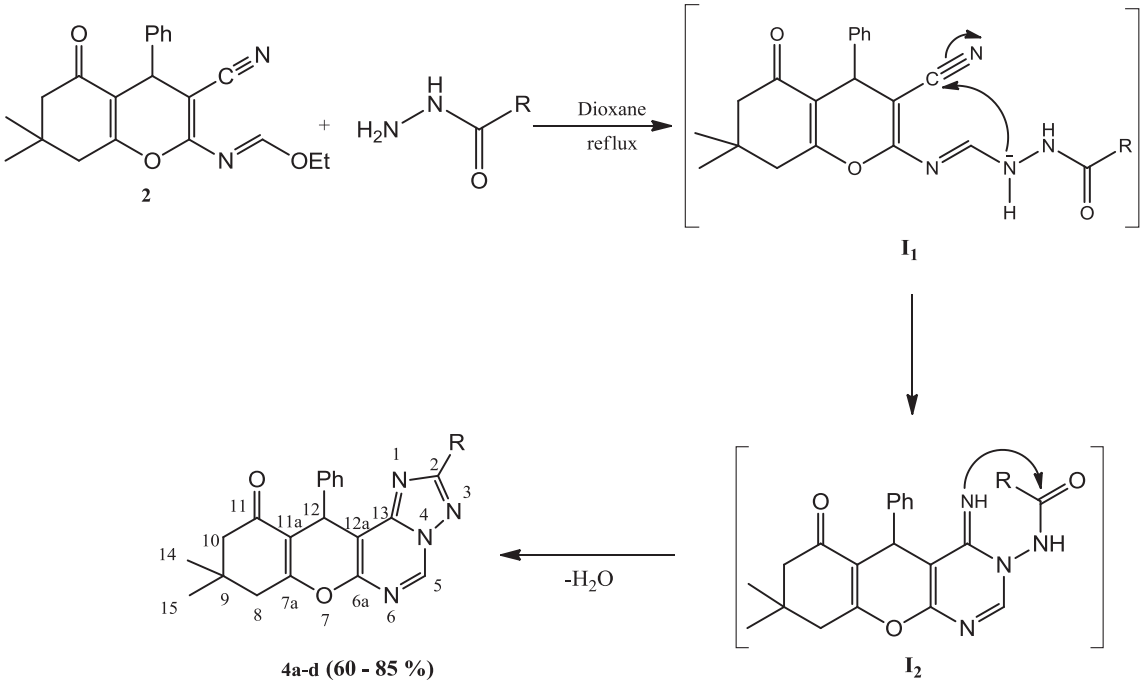

Fig. 3. Target compounds.

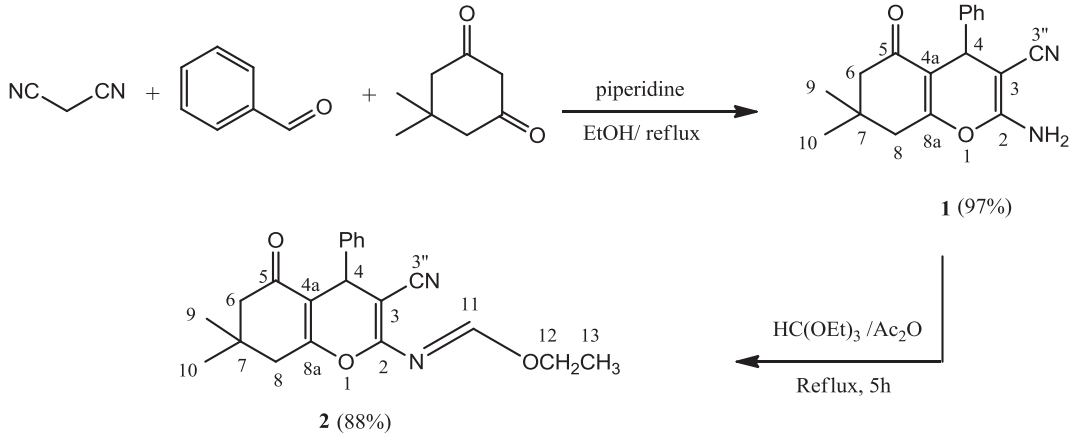

Scheme 1. Synthetic pathway to the precursors **1** and **2.**

Table 1
Synthesis of pyranopyrimidines **3a-f.**

	3a	3b	3c	3d	3e	3f
Ar	Ph	3-CH_3Ph	4-C_2H_5Ph	3-ClPh	4-OCH_3Ph	1-naphthyl
Yield (%)	67	74	80	76	86	84

exerted a mesomeric donor effect whereas chlorine atom exerted both a mesomeric donor and an inductive attractor effects. The derivative **3a** (Ph) (aPTT = 57.1 ± 0.7 s) displayed an anticoagulant capacity slightly higher than **3b** (3-CH_3Ph) and **3d** (3-ClPh). This result shows the ineffectiveness of these two substituents in the aryl group at 3-position compared to the hydrogen atom.

On the other hand, the pyranotriazolopyrimidines **4a-d** (aPTT = 55.1.0 ± 1.1 – 63.4 ± 0.7 s) were found to be anticoagulant compared to the negative control (plasma). The derivative **4c** (R = CH_2CN) exhibited the highest activity with an aPTT value of 63.4 ± 0.7 s followed by **4b** (R = CH_3) (aPTT = 60.1 ± 1.2 s). The comparison of the anticoagulant activity of **4b** and **4c** with that of the non substituted triazole derivative **4a** (aPTT = 59.4 ± 0.8 s) does not show the impact of these two substituents introduced (CH_3 and CH_2CN) to improve this activity. Moreover, the coumarin moiety in compound **4d** (aPTT = 55.1 ± 1.1 s) did not seem to bring any anticoagulant activity by comparison to **4a**. This result could be explained by the extension of the size of the molecule and the decrease of its polarity which influence its solubility. All the tested compounds remain less active than heparin (aPTT = 125.2 ± 3.8 s, cc = 10 µg/mL) used as positive control.

2.2.2. *Anti-tyrosinase activity*

Tyrosinase is an enzyme present in the skin that activates the transformation of tyrosine (amino acid) into dark-colored pigment melanin. Its absence or mutation of its gene lead to a decrease or even a halting of the pigmentation. The *in vitro* anti-tyrosinase activity of compounds **1**, **2**, **3a-f** and **4a-d** were assessed by measuring the inhibition percentage (PI %). The results presented in Table 3 showed that most of tested compounds displayed significant anti-tyrosinase activity with percent of inhibition ranging from 73.77 ± 1.10 to 98.84 ± 1.81% compared to that of kojic acid used as a positive control (85.50 ± 1.00%). It has been found that the iminoether **2**

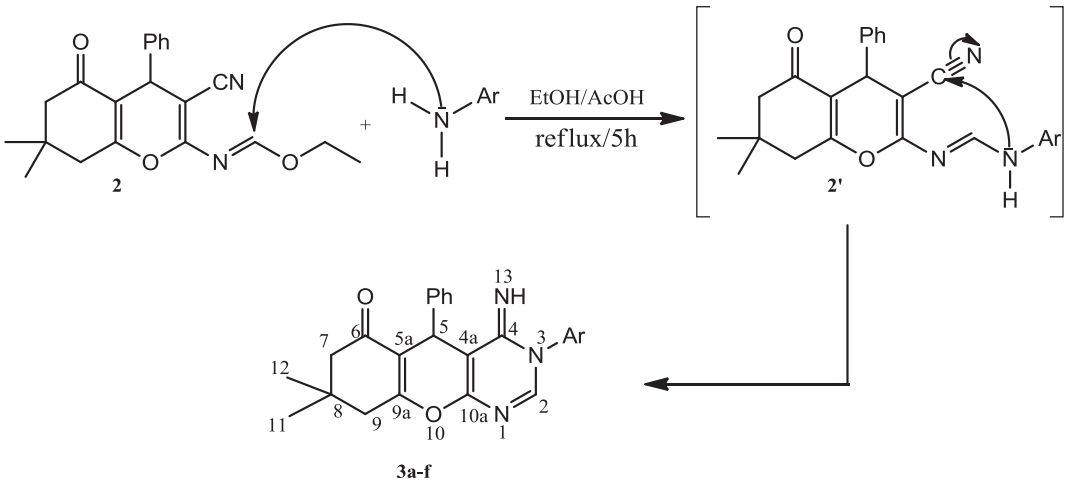

Scheme 2. Synthetic pathway of pyranopyrimidines **3a-f.**

exhibited the highest tyrosinase inhibitor with a PI value of 98.84 ± 1.81% whereas the starting compound **1** was the less active one against tyrosinase (PI = 73.77 ± 1.10%), hence the importance to modify the primary amine function into imine.

On the other hand, from the series of compounds **3a-f**, only **3a**, **3c** and **3d** displayed anti-tyrosinase capacity with PI values of 91.35 ± 1.00, 84.14 ± 2.00 and 94.23 ± 1.45%, respectively. It is clear that the chlorine atom and its 3-position of the aromatic ring were in favor of the high activity of compound **3d**. These results show that the attachment of a methyl group at the 3-position on the aromatic ring (compound **3b**) results in the loss of activity compared with compound **3a** with an unsubstituted aromatic ring (PI = 91.35 ± 1.00%), whereas, the introduction of an ethyl group at the 4-position of the aromatic ring in compound **3c** has generated an interesting anti-tyrosinase activity (PI = 84.14 ± 2.00%).

The inactivity of compound **3e** (4-OCH_3Ph) compared to its bioactive analogue **3c** (4-C_2H_5Ph) clearly shows the importance of the nature of the substituent attached to the 4-position of the aromatic ring in addition to the electronic effects (+I and/or +M) that can apply. The inactivity of the compound **3f** (naphtyl) compared to its analogue **3a** (Ph) (PI = 91.35 ± 1.00%) suggests that the extension of the conjugation might not be in favor of this activity. The difference in size and spatial arrangement between these two molecules could also be at the origin of the total loss of this activity by replacing a phenyl by a naphthyl group.

Table 2
Synthesis of pyranotriazolopyrimidines **4a-d.**

	4a	4b	4c	4d
R	H	CH_3	CH_2CN	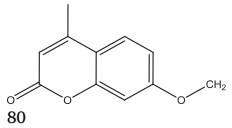
Yield (%)	85	60	73	80

On the other hand, only the compound **4b** (R = CH_3) was found to be inactive towards tyrosinase enzyme. Compound **4c** (R = CH_2CN) exhibited the highest activity (PI = 93.94 ± 1.58%) followed by **4d** with a coumarin system attached to its triazole ring

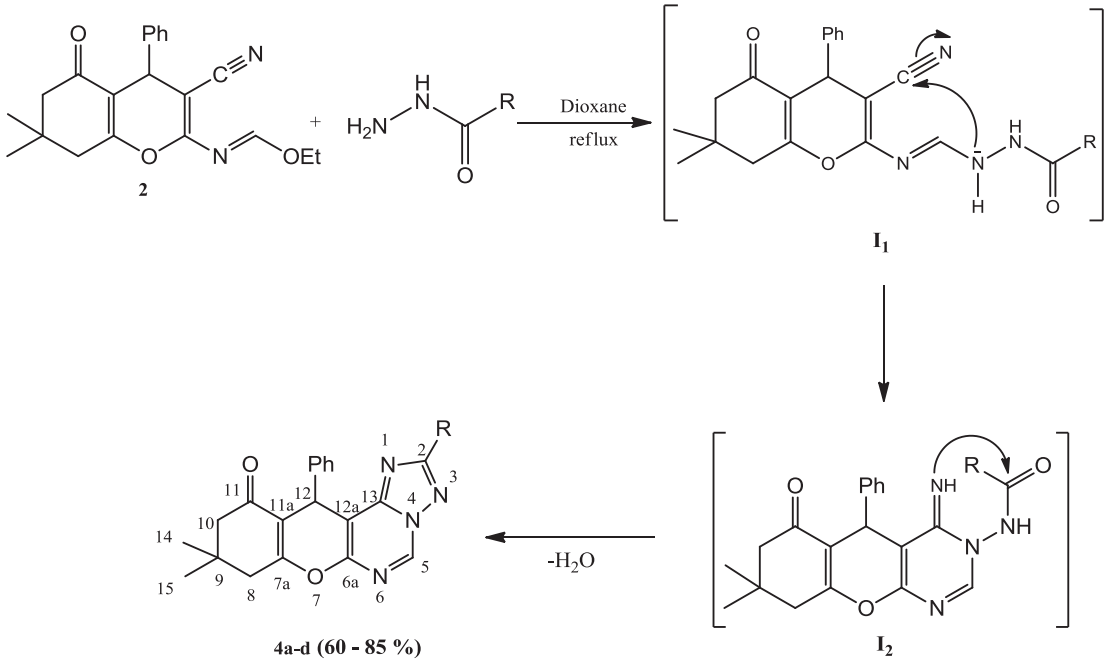

Scheme 3. Synthetic pathway of pyranotriazolopyrimidines **4a-d.**

Table 3
Anticoagulant and anti-tyrosinase activities of compounds **1**, **2**, **3a-f** and **4a-d.**

Compounds	aTTP (s)[a]	(PI%)[b]
1	68.3 ± 0.8	73.77 ± 1.10
2	72.8 ± 0.9	98.84 ± 1.81
3a	57.1 ± 0.7	91.35 ± 1.00
3b	53.7 ± 0.9	na[c]
3c	61.8 ± 1.0	84.14 ± 2.00
3d	54.8 ± 0.8	94.23 ± 1.45
3e	57.0 ± 1.0	na
3f	63.2 ± 1.1	na
4a	59.4 ± 0.8	78.09 ± 0.94
4b	60.1 ± 1.2	na
4c	63.4 ± 0.7	93.94 ± 1.58
4d	55.1 ± 1.1	90.12 ± 2.10
Plasma[d]	33.50 ± 0.05	
Heparin[e]	125.2 ± 3.8	
Kojic acid[f]		85.50 ± 1.00

[a] Expressed by measuring the activated Partial Thromboplastin Time (aPTT) (s) at the concentration of 1000 µg/mL and was the mean of three replicates (mean ± SD, n = 3).
[b] Capacities were represented as percent of inhibition (mean ± SD, n = 3).
[c] Non active.
[d] Negative control.
[e] Positive control at the concentration of 10 µg/mL.
[f] Positive control.

(PI = 90.12 ± 2.10%). The electron-withdrawing cyano group in compound **4c** is certainly at the origin of the high activity compared to that of compound **4a** where this group is replaced by a hydrogen atom (PI = 78.09 ± 0.94%). The compounds **4c** and **4d** were found more effective than the positive control (PI = 85.50 ± 1.00%). These findings reveal the importance of the nature of the substituent borne by the triazole.

2.2.3. Molecular docking studies

Tyrosinase is a binuclear copper-containing enzyme that catalyzes the conversion of a monophenol (tyrosine) and/or o-diphenol (L-DOPA) in its corresponding o-qunione derivative. The crystal structure is mainly composed tetramer subunit chain-A, chain-B, Chain- C and chain- D, respectively with the sequence length of 391 [32].

In depth docking analysis has been performed and investigation were carried out to elucidate the interaction of this class of scaffolds within the hydrophobic binding pocket of tropolone in PDB: 2Y9X and to investigate the binding mode and binding energies of **1**, **2**, **3a**, **3b**, **3c**, **3d**, **3e**, **3f**, **4a**, **4b**, **4c** and **4d** (Table 4) at the tropolone binding domain of binuclear copper containing enzyme (PDB: 2Y9X) by using auto dock 4.2. The majority of anti-tyrosinase agents that targets the tropolone binding site, reported thus far, resemble the binding interaction of tropolone within the hydrophobic binding site. Amongst all designed scaffolds most active set of compounds in terms of binding energies are within the conjugates **2**, **3a**, **3b**, **3c** and **3d** found to be most active in terms of binding energy and interactions within the tropolone binding cavity of PDB: 2Y9X (Figs. 4 and 5).

In depth structure activity relationship of anti-tyrosinase agents

Table 4
Binding energies of promising anti-tyrosinase agents.

Binding Energy (kcal/mol)						
Tropolone	−5.33	−5.22	−5.18	−5.18	−4.95	−5.01
1	−8.20	−8.12	−8.09	−8.09	−8.04	−7.93
2	−9.20	− 9.18	− 8.71	−8.70	−8.49	− 9.20
3a	−9.12	−9.20	−9.00	−9.50	−9.20	− 9.12
3b	**−9.37**	**−9.16**	**−9.04**	**−8.91**	**−8.41**	**−9.37**
3c	**−9.50**	**−9.45**	**−9.10**	**−8.63**	**−8.46**	**−8.46**
3d	**−9.95**	**−9.89**	**−9.80**	**−9.71**	**−9.69**	**−9.23**
3e	−7.01	−6.72	−6.57	−6.36	−7.00	−7.00
3f	−7.95	−7.89	−7.80	−7.72	−7.71	−7.57

(Fig. 5) suggest that " 4-imino-8,8-dimethyl-3,5-diphenyl-5,7,8,9-tetrahydro-3H-chromeno[2,3-*d*]pyrimidin-6(4H)-one" core with ring A, B, C, D and E is most essential platform for the design of conjugates **3a**, **3b**, **3c**, **3d**, **3e** and **3f**. In conclusion, we observed that dimethyl group at position 8 of basic pharmacophore is essential for pi-alkyl type of interaction with surrounding amino acid sequence within the binding cavity of tropolone in addition to this 4-imino functional group gives it a unique character to get ionized and form hydrogen bonds with pocket amino acids (Fig. 6). Basic pharmacophore is a blend of saturated and unsaturated system which is essential for the pi-pi and pi-alkyl interactions which may be responsible for anti-tyrosinase property. Coming to diphenyl ring substitution at position 3 and 5 (most essential) respectively suggests that aliphatic substitutions in phenyl ring E may explore probability to have promising anti-tyrosinase activity and binding interactions, but in contrast bulkier ring or extension of this 3-ring pharmacophore to 4 ring system is a demerit for binding energies which we observed for conjugates **4a**, **4b**, **4c** and **4d**, respectively.

Binding site of conjugate **3d** (most effective anti-tyrosinase agent from the series **3**) in hydrophobic cavity of PDB: 2Y9X (Fig. 7), 2D-interactions in between 4 and imino group and some unfavorable bumps in red color code with GLU-A-98 (conventional hydrogen bond interactions in green color), Chlorine substitution in ring E is involved in conventional hydrogen bond interaction with TRP-A-293 (green color) and some unfavorable bumps (red color) with TRP-A-293, PHE-A-292 were observed due to Pi-Pi electron clouds in ring E, apart from this Pi-alkyl interactions were observed with TYR-A-9 in ring E, some more unfavorable bumps were observed with GLU-A-98, ARG-A-95, ASP-A-300 (Pi-anion in golden color), LEU-A-303 and VAL-A-299, respectively. Phenyl ring D is involved in Pi-Pi interactions with ARG-A-95 similarly some Pi-alkyl, Pi—Pi and conventional bonds were observed in Ring A with PRO-A-91, VAL-A-299, PHE-A-241 and LEU-A-255, respectively.

3. Conclusion

In this paper we have synthesized a series of new pyranopyrimidine- and pyranotriazolopyrimidine-based bioactive heterocyclic compounds **3** and **4** by reacting the α-functionalized-iminoether **2**, previously prepared from α-aminocarbonitrile **1**, with a series of primary aromatic amines and hydrazides, respectively. The newly prepared compounds **3a-f** and **4a-d** have been tested for their possible anticoagulant and anti-tyrosinase activities. The results showed that most compounds exhibited interesting activity and in depth docking analysis reveals the structure activity relationship which is relevant with the findings of biological evaluations. It has been found that the iminoether **2** exhibited the highest anticoagulant activity and tyrosinase inhibition amongst all compounds synthesized and tested. Most pyranopyrimidines **3** and pyranotriazolopyrimidines **4** also displayed interesting activity In depth docking analysis leads to a conclusion that 4-imino-8,8-dimethyl-3,5-diphenyl-5,7,8,9-tetrahydro-3H-chromeno[2,3-*d*]pyrimidin-6(4H)-one is absolutely important for buildup and improvement of antityrosinase activity of conjugates. Insilico SAR studies were supported with biological evaluation and in most of the cases the SAR showed the nature and the electron effect of the substituents on the aromatic ring or on the triazole moiety of pyranopyrimidines **3** and pyranotriazolopyrimidines **4**, respectively to improve and to show significant binding interaction proven with Insilico docking studies.

4. Materials and methods

4.1. Chemistry

All reactions were monitored by TLC using aluminium sheets of Merck silica gel 60 F_{254}, 0.2 mm. Melting points were determined on a Büchi 510 apparatus using capillary tubes.

NMR spectra were recorded on a Bruker AC-300 spectrometer at

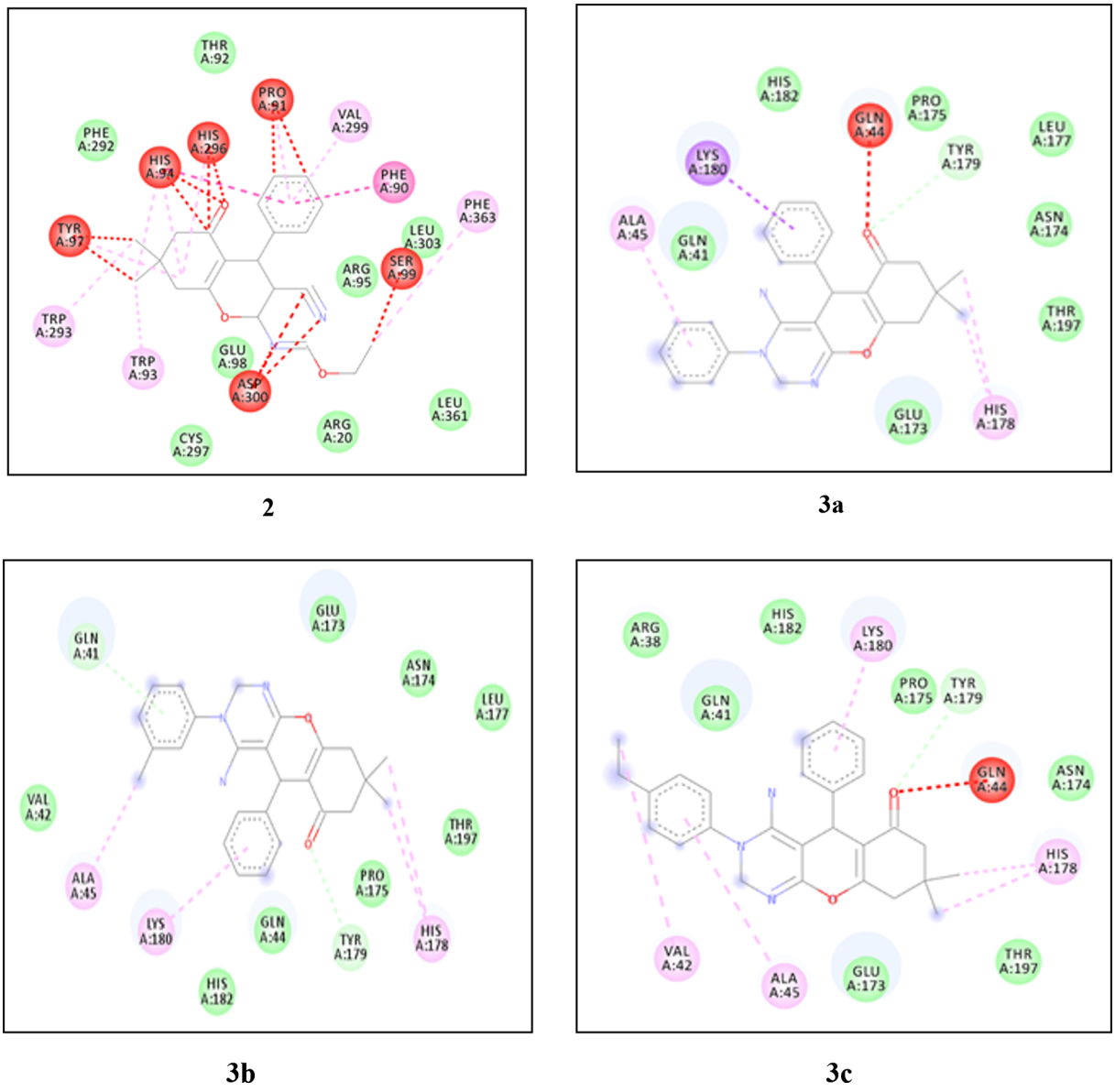

Fig. 4. Binding pose of conjugates **2, 3a, 3b and 3c** in the tropolone binding cavity of PDB: 2Y9X.

300 MHz (^{1}H) and 75 MHz (^{13}C). All chemical shifts were reported as δ values (ppm) relative to residual non deuterated solvent and coupling constants (*J*) in Hertz. Mass spectra were obtained with ESI-TOF (LCT, Waters) using the reflectron mode in the positive ion mode.

*4.1.1. General procedure for the synthesis of 2-amino-3-cyanopyranes **1***

To a stirred stoichiometric mixture of arylaldehyde (10 mmol), malononitrile (10 mmol) and 5,5-dimethylcyclohexane-1,3-dione (10 mmol) in absolute ethanol (30 mL) was added a catalytic amount of piperidine and then was refluxed for 2 h. The solid product formed is filtered, dried and purified by recrystallization from ethanol to give compound **1** in good yield 97%.

*4.1.1.1. 2-amino-9,10-dimethyl-5-oxo-4-phenyl-5,6,7,8-tetrahydro-4H-chromene-carbonitrile **1**.* White solid, yield 97%, m.p: 240 °C, ^{1}H NMR ($CDCl_3$,300 MHz) δ_H: 1.04 (3H, s, H_9), 1.11 (3H, s, H_{10}), 2.21 (2H, s, H_8), 2.45 (2H, s, H_6), 4.41(1H, s, H_4), 4.51 (2H, s, NH_2),7.26 (5H, s, H_{arom}). ^{13}C NMR ($CDCl_3$, 75 MHz) δ_C: 27.6, 28.7, 32.11, 35.5, 40.7, 50.7, 63.9, 114.2, 118.3, 157.5, 161.3, 195.5.

*4.1.2. General procedure for the synthesis of the α-functionalized iminoether **2***

The mixture of **1** (0.01 mmol) and triethylorthoformate (0.01 mmol) in acetic anhydride (30 mL) was refluxed for 1 h. The solvent was then removed under reduced pressure. The remaining solid was re-crystallized from ethanol to give compound **2**.

4.1.2.1. EthylN-(3-cyano-7,7-dimethyl-5-oxo-4-phenyl-5,6,7,8-tetrahydro-4H-chromen-2-yl) formimidate 2. White solid, yield: 88%, m.p: 148 °C, ^{1}H NMR ($CDCl_3$, 300 MHz) δ_H: 1.03–1.05 (6H, 4 s, H_9, H_{10}), 1.36 (3H, t, J = 6.9 Hz, H_{13}), 2.25 (2H, d, J = 16.5 Hz, H_8), 2.53 (2H, d, J = 12 Hz, H_6) 4.41 (2H, q, J = 6.9 Hz, H_{12}), 4.61 (1H, s, H_4), 7.16–7.92 (5H, m, H_{arom}), 8.21 (1H, s, H_{11}). ^{13}C NMR ($CDCl_3$, 75 MHz) δ_C: 13.2, 27.1, 28.2, 31.6, 35.1, 40.3, 50.2, 63.8, 83.4, 112.6, 126.5, 128.3, 155.4, 160.3, 161.5, 195.0, 126.8.

*4.1.3. General procedure for the synthesis of the pyranopyrimidines **3a-f***

The appropriate primary amine (0.001 mol) was added to the iminoether **2** (0.001 mol), and the mixture was stirred at reflux of ethanol (20 mL) and a few drops of acetic acid for 6 h. After cooling, the

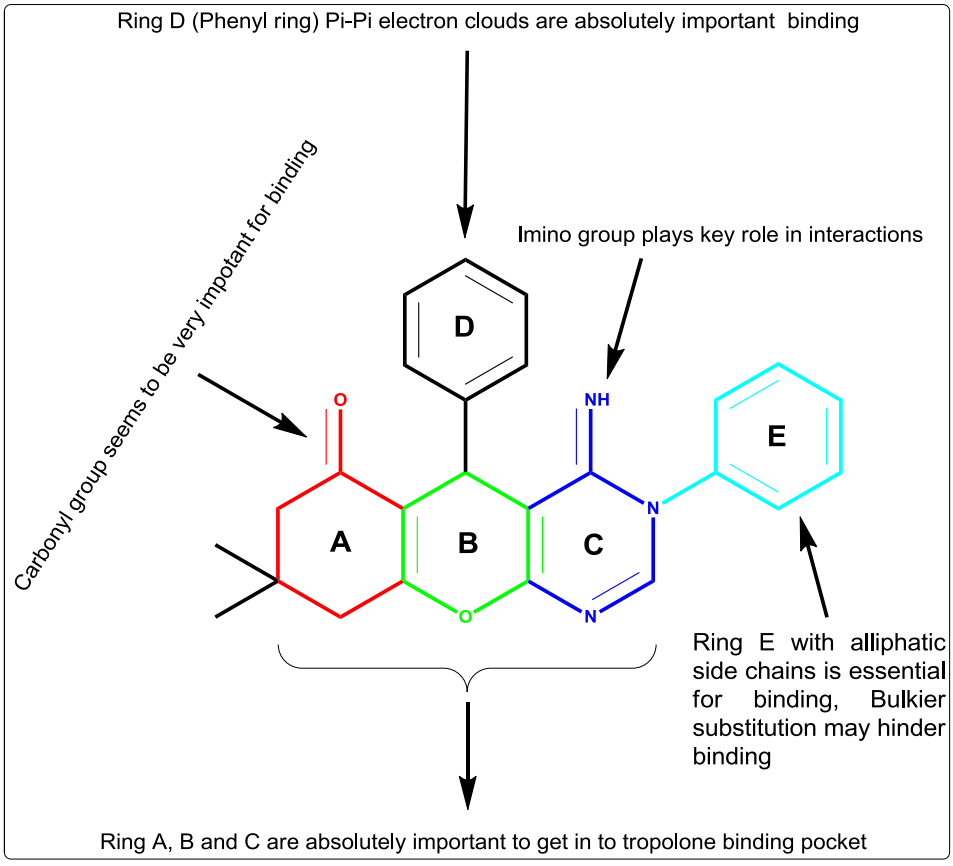

Fig. 5. Structure activity relationship of designed scaffolds for anti-tyrosinase agents.

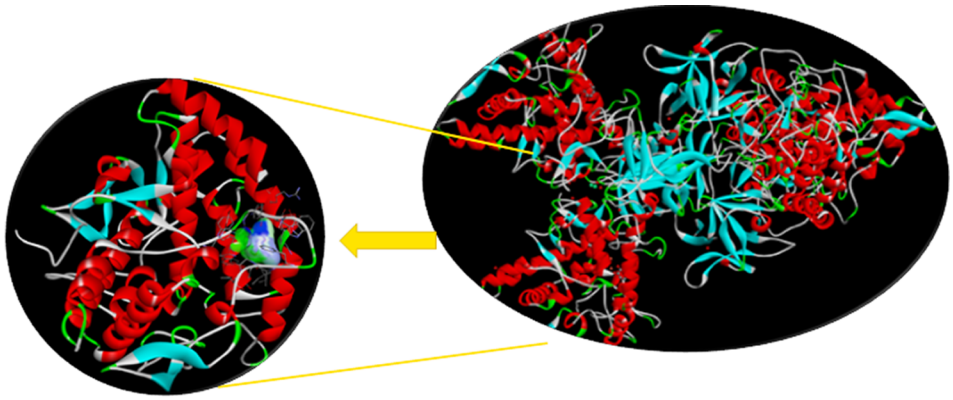

Fig. 6. Binding site of tropolone in hydrophobic cavity of PDB: 2Y9X, 2D-interactions with ALA-A-221 (Vander waal interactions in green color), hydrophobic cavity composed of surrounding amino acids sequence ALA-A-220, LEU-A-265, ILE-A-217, TRP-A-136, TRP-A-138, GLY-A-149, PHE-A-147, TYR-A-140, ASP-A-137, TRP-A-141 and PHE-A-224, respectively.

precipitated solid was filtered, washed with cold ethanol, and dried to obtain compounds **3a-f**.

4.1.3.1. 4-imino-8,8-dimethyl-3,5-diphenyl-5,7,8,9-tetrahydro-3H-chromeno[2,3-d]pyrimidin-6(4H)-one ***3a***. Yellow solid, yield: 67%, m.p: 254 °C. ESI-HRMS $[M+H]^+$calcd. for $(C_{25}H_{24}N_3O_2)^+$: 398.1869, found: 398.1888. ^{1}H NMR (DMSO-d_6, 300 MHz) δ_H: 0.97–1.07 (6H, 2 s, H_{11+12}), 2.19 (1H, d, J = 16.2 Hz, H_{9a}), 2.35 (1H, d, J = 16.2 Hz, H_{9b}), 2.57 (1H, d, J = 17.7 Hz, H_{7a}), 2.65 (1H, d, J = 17.7 Hz, H_{7b}), 5.45 (1H, s, H_5), 6.99–7.54 (10H, m, H_{arom}), 8.28 (1H, s, H_2), 8.60 (1H, s, H_{13}). ^{13}C NMR (DMSO-d_6, 75 MHz) δ_C: 26.5, 28.5, 31.4, 31.8, 39.4, 50.15, 121.7, 128.2, 99.72, 114.27, 155.9, 158.9, 161.4, 163.7, 195.5.

4.1.3.2. 4-imino-8,8-dimethyl-3,5-diphenyl-5,7,8,9-tetrahydro-3H-chromeno[2,3-d] pyrimidin-6 (4H) –one ***3b***. White solid, yield: 74%, m.p: 172 °C. ESI-HRMS $[M+H]^+$calcd. for $(C_{26}H_{26}N_3O_2)^+$: 412.2025 found 412.2045. ^{1}H NMR ($CDCl_3$, 300 MHz) δ_H: 1.01–1.12 (6H, 2 s, H_{12}, H_{11}), 2.29 (2H, d, J = 5.4 Hz, H_9), 2.31 (3H, s, C$\underline{H}_3$-Ph), 2.61 (2H, s, H_7), 4.89 (1H, s, H_5), 6.31 (1H, s, H_2), 6.98–7.47 (9H, m, H_{arom}), 8.42 (1H, s, H_{13}). ^{13}C NMR ($CDCl_3$, 75 MHz) δ_C: 20.8, 26.9, 28.3, 31.65, 33.9, 40.6, 50.2, 98.4, 113.8, 118.1–128.6, 155.9, 158.9, 160.7, 162.6, 195.5.

4.1.3.3. 3-(4-ethylphenyl)-4-imino-8,8-dimethyl-5-phenyl-5,7,8,9-tetrahydro-3Hchromeno[2,3-d] pyrimidin-6(4H)–one ***3c***. Yellow solid, yield: 80%, m.p: 202 °C. ESI-HRMS $[M+H]^+$ calcd. for $(C_{27}H_{28}N_3O_2)^+$: 426.2182 found 426.2203. ^{1}H NMR ($CDCl_3$, 300 MHz) δ_H: 1.01–1.19 (6H, 2 s, H_{11}, H_{12}), 1.29 (2H, d, J = 6.6 Hz, H_9), 2.25 (2H, s, H_7), 2.67 (3H, s, C$\underline{H}_3$-C$\underline{H}_2$-Ph), 4.92 (1H, s, H_5), 6.67 (1H, s, H_2), 7.15–7.49 (9H, m, H_{arom}), 8.42 (1H, s, H_{13}). ^{13}C NMR ($CDCl_3$, 75 MHz) δ_C: 15.4, 27.4, 28.8, 28.2, 32.1, 34.4, 41.2, 50.7, 98.7, 114.3, 121.7, 129.1, 156.6, 159.6, 161.2, 163.1, 196.0.

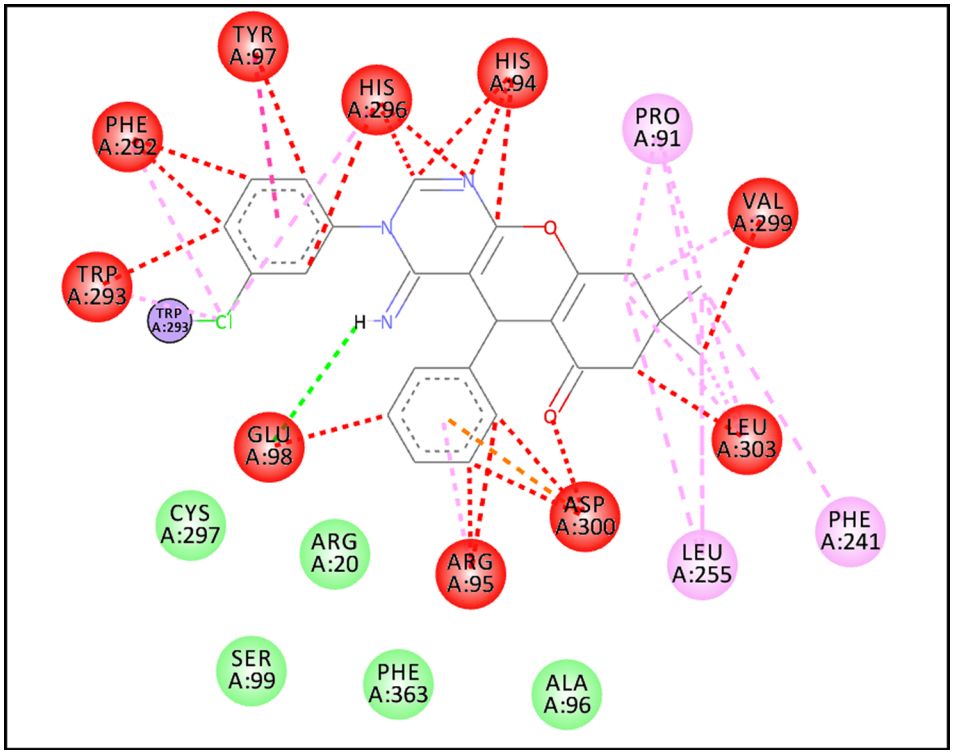

Fig. 7. Binding site of conjugate **3d** (most effective anti-tyrosinase agent) in hydrophobic cavity of PDB: 2Y9X and 2D-interactions.

4.1.3.4. (3-chlorophenyl)-4-imino-8,8-dimethyl-5-phenyl-5,7,8,9-tetrahydro-3Hchromeno[2,3-d]pyrimidin-6 (4H)–one ***3d***. White solid, yield: 76%, m.p: 164 °C. ESI-HRMS $[M+H]^+$calcd. for $(C_{25}H_{23}ClN_3O_2)^+$: 432.1479 found 432.1498. ^1H NMR ($CDCl_3$, 300 MHz) δ_H: 1.01–1.12 (6H, 2 s, H_{12}, H_{11}), 2.25 (2H, s, H_9), 2.66 (2H, s, H_7), 3.78 (1H, s, H_{13}), 4.95 (1H, s, H_5), 6.68–7.54 (9H, m, H_{arom}), 8.47 (1H, s, H_2). ^{13}C NMR ($CDCl_3$, 75 MHz) δ_C: 26.8, 28.3, 31.6, 33.8, 40.6, 50.2, 98.9, 113.7, 118.4–129.7, 156.1, 158.6, 160.9, 162.6, 195.5.

4.1.3.5. 4-imino-3-(4-methoxyphenyl)-8,8-dimethyl-5-phenyl-5,7,8,9-tetrahydro-3H-chromeno [2,3-d] pyrimidin-6 (4H) –one ***3e***. Yellow solid, yield: 86%, m.p: 218 °C. ESI-HRMS $[M+H]^+$calcd. for $(C_{26}H_{26}N_3O_3)^+$: 428.1974 found 428.1994. ^1H NMR ($CDCl_3$, 300 MHz) δ_H: 1.02–1.19 (6H, 2 s, H_{11}, H_{12}), 2.19 (2H, s, H_9), 2.65 (2H, s, H_7), 3.78 (3H, s, OCH_3), 4.95 (1H, s, H_5), 6.50–7.45 (9H, m, H_{arom}), 8.39 (1H, s, H_2). ^{13}C NMR ($CDCl_3$, 75 MHz) δ_C: 26.9–28.3, 31.6, 33.8, 40.7, 50.2, 54.9, 98.02, 113.7, 123.2, 130.4, 156.4, 159.3, 160.7, 162.7, 195.6.

4.1.3.6. 4-imino-8,8-dimethyl-3-(naphthalen-1-yl)-5-phenyl-5,7,8,9-tetrahydro-3H-chromeno [2,3-d] pyrimidin-6 (4H) –one ***3f***. White solid, yield: 84%, m.p: 234 °C. ESI-HRMS $[M+H]^+$calcd. for $(C_{29}H_{26}N_3O_2)^+$: 448.2025 found 448.2045. ^1H NMR ($CDCl_3$, 300 MHz) δ_H: 1.00–1.19 (6H, 2 s, H_{12}, H_{11}), 2.22 (2H, s, H_9), 2.65 (2H, s, H_7), 5.12 (1H, s, H_5), 6.81–7.87 (12H, m, H_{arom}), 8.35 (1H, s, H_2), 7.43 (1H, s, H_{13}). ^{13}C NMR ($CDCl_3$, 75 MHz) δ_C: 27.0–28.2, 31.6, 34.0, 40.7, 50.3, 98.02, 113.7, 120.6, 128.8, 156.4, 159.3, 160.7, 162.7, 195.6.

4.1.4. General procedure for the synthesis of the pyranotriazolopyrimidines ***4a-d***

Equimolar solution (15 mmol) of imino ether **2** and hydrazide was refluxed in dry dioxane (40 mL) with continuous stirring for 24 h under argon atmosphere. The crude product was purified by column chromatography (PE:EtOAc 4:6) to give compound **4a-d**.

4.1.4.1. 9,9-dimethyl-12-phenyl-9,10-dihydro-8H-chromeno[3,2-e][1,2,4]triazolo[1,5-c]pyrimidin-11(12H)-one ***4a***. White solid, yield: 85%, m.p: 223 °C. ESI-HRMS $[M+H]^+$calcd. for $(C_{20}H_{19}N_4O_2)^+$: 347.1508 found 347.1530. ^1H NMR ($CDCl_3$, 300 MHz) δ_H: 1.08–1.10 (6H, 2 s, H_{14}, H_{15}), 2.19 (2H, d, J = 16.2 Hz, H_{8a}), 2.29 (2H, d, J = 16.2 Hz, H_{8b}), 2.58 (2H, d, J = 3 Hz, H_{10a}), 2.69 (2H, d, J = 3 Hz, H_{10b}), 5.43 (1H, s, H_{12}), 7.05–7.39 (5H, m, H_{arom}), 8.23(1H, s, H_5), 9.04 (1H, s, H_2). ^{13}C NMR ($CDCl_3$, 75 MHz) δ_C: 27.5, 29.0, 32.3, 34.7, 41.1, 50.7, 105.4, 113.5, 127.3, 128.5, 138.5, 152.3, 156.9, 152.7, 163.6, 195.9.

4.1.4.2. 2,9,9-trimethyl-12-phenyl-9,10-dihydro-8H-chromeno[3,2e][1,2,4] triazolo[1,5-c]pyrimidin-11(12H)–one ***4b***. White solid, yield: 60%, m.p: 226 °C. ESI-HRMS $[M+H]^+$ calcd. for $(C_{21}H_{21}N_4O_2)^+$: 361.1665 found 361.1684. ^1H NMR ($CDCl_3$, 300 MHz) δ_H: 1.10–1.16 (6H, 2 s, H_{15}, H_{14}), 2.24 (2H, d, J = 16.2 Hz, H_{8a}), 2.36 (2H, d, J = 16.2 Hz, H_{8b}), 2.53 (3H, s, CH_3), 2.61 (2H, d, J = 17.7 Hz, H_{10a}), 2.75 (2H, d, J = 17.7 Hz, H_{10b}), 5.49 (1H, s, H_{12}), 7.13–7.45 (5H, m, H_{arom}), 8.97 (1H, s, H_5). ^{13}C NMR ($CDCl_3$, 75 MHz) δ_C: 27.0, 28.5, 14.04, 31.75, 34.0, 40.7, 50.2, 104.0, 126.6, 127.8, 113.3, 137.6, 152.3, 152.4, 163.0, 167.2, 195.0.

4.1.4.3. 2-(9,9-dimethyl-11-oxo-12-phenyl-9,10,11,12-tetrahydro-8H-chromeno[3,2-e][1,2,4] triazolo [1,5- c] pyrimidin-2-yl) acetonitrile ***4c***. White solid, yield: 73%, m.p: 228 °C. ESI-HRMS $[M+H]^+$calcd. for $(C_{22}H_{20}N_5O_2)^+$: 386.1617 found 386.1636. ^1H NMR ($CDCl_3$, 300 MHz) δ_H: 1.14–1.25 (6H, 2 s, H_{14}, H_{15}), 2.29 (2H, d, J = 16.5 Hz, H_{8a}), 2.39 (2H, d, J = 16.5 Hz, H_{8b}), 2.65 (2H, d, J = 17.7 Hz, H_{10a}), 2.78 (2H, d, J = 17.7 Hz, H_{10b}), 3.99 (2H, s, CH_2), 5.49 (1H, s, H_{12}), 7.13–7.84 (5H, m, H_{arom}), 9.06 (1H, s, H_5). ^{13}C NMR ($CDCl_3$, 75 MHz) δ_C: 24.3, 27.5, 18.6, 32.2, 34.6, 41.1, 50.7, 105.3, 113.6, 114.4, 138.1, 127.3, 128.4, 153.5, 160.9, 163.5, 163.8, 195.5.

4.1.4.4. 9,9-dimethyl-2-(((4-methyl-2-oxo-2H-chromen-7-yl) oxy) methyl) -12-phenyl-9,10-dihydro-8H-chromeno [3,2 e] [1,2,4] triazolo [1,5-c] pyrimidin-11 (12H) –one ***4d***. White solid, yield: 80%, m.p: 225 °C. HRMS $[M+H]^+$calcd. for $(C_{31}H_{27}N_4O_5)^+$: 535.1981 found 535.2002.

^{1}H NMR ($CDCl_3$, 300 MHz) δ_H: 1.11–1.19 (6H, 2 s, H_{14}, H_{15}), 2.24 (2H, d, J = 16.2 Hz, H_{8a}), 2.37 (2H, d, J = 16.2 Hz, H_{8b}), 2.39 (3H, s, C$\underline{H}_3$), 2.61 (2H, d, J = 4.8 Hz, H_{10a}), 2.79 (2H, d, J = 4.8 Hz, H_{10b}), 5.39 (2H, s, OC$\underline{H}_2$), 5.51 (1H, s, H_{12}), 6.92–7.49 (8H, m, H_{arom}), 9.04 (1H, s, H_5). ^{13}C NMR ($CDCl_3$, 75 MHz) δ_C: 17.9, 27.0, 28.4, 31.7, 34.1, 40.6, 50.2, 63.5, 101.9, 104.9, 113.8, 127.9, 137.8, 152.5, 152.9, 160.6, 163.0, 164.9, 195.0.

4.2. Biological evaluation

4.2.1. Anticoagulant activity

The anticoagulant activity of the synthesized compounds were evaluated by measuring the aPTT (Thromboplastin partial activation time) using Platelin LS reagent (Trinity Biotech PLC, Cowicklow, Ireland). The coagulation test was carried out using normal human citrate plasma poor in platelets. In a coagulometer bowl, 45 µL of normal citrate plasm pool containing 5 µL of the tested product solution at concentrations of 1000 µg/mL are incubated for 1 min at 37 °C, 50 µL of Platelin LS activator are then added. After 3 min incubation at 37 °C, 50 µL of previously heated $CaCl_2$ 0.025 M are also added. The time of appearance of the clot is measured by the coagulometer, Heparin (10 µg/mL) was used as positive control and the test was conducted in triplicate [33].

4.2.2. Antityrosinase activity

The mushroom tyrosine inhibition effect was determined using L-tyrosine (1 mM) as the substrate. Hydroquinone (1 mM) was used as a tyrosinase inhibitor. The substrate and inhibitor were prepared in 0.1 M phosphate buffer pH 6.5. Inhibition of tyrosinase was tested in a reaction mixture (4 mL) consisting of 1.960 mL of phosphate buffer, 2 mL of L-tyrosine (1 mM), 20 µL of fungus tyrosinase and 20 µL of hydroquinone (1 mM). The reaction was initiated by adding enzyme to the substrate solution and the inhibitor. The reaction and all solutions were thermostated at 25 °C. The effect of inhibition was determined by the maximum decrease in the amount of dopachrome formed and the absorbance was measured by spectrophotometry at 475 nm, a wavelength at which all the compounds tested do not absorb. A blank assay (without tyrosinase) was conducted. The test was performed in triplicate. The percentage inhibition of tyrosinase activity at the concentration of 100 µM was calculated according to the equation: (%) = ((A − B)/A) × 100 where A represents the optical density of the enzyme tyrosinase and B represents the optical density of the product tested for 30 min [34].

4.2.3. Molecular docking procedure

The optimization of all the geometries is carried out in Gaussian 09 using PM3 semi-empirical method [35]. The crystal structures of PDB (PDB: 2Y9X) were obtained from the RSCB protein data bank [32]. Docking studies were performed using AutoDock 4.2 software [36]. The Analysis of intermolecular interactions has been performed using Pymol, v. 0.99 [37].

Declaration of interest

The authors declare no conflicts of interests. The authors alone are responsible for the content and writing of this article.

Appendix A. Supplementary material

Supplementary data to this article can be found online at https://doi.org/10.1016/j.bioorg.2018.10.004.

References

[1] W. Benjamin, T.J.J. Müller, Regioselective three-component synthesis of highly fluorescent 1,3,5-trisubstituted pyrazoles, Eur. J. Org. Chem. 2008 (2008) 4157–4168.

[2] M. Adib, E. Sheikhi, A. Kavoosi, H.R. Bijanzadeh, Synthesis of 2-(alkylamino)-5-{alkyl[(2-oxo-2*H*-chromen-3-yl)carbonyl]amino}-3,4-furandicarboxylates using a multi-component reaction in water, Tetrahedron 66 (2010) 9263–9269.

[3] S.A. Said, A.E.G. Amr, N. Sabry, M.M. Abdalla, Analgesic, anticonvulsant and anti-inflammatory activities of some synthesized benzodiazipine, triazolopyrimidine and bis-imide derivatives, Eur. J. Med. Chem. 44 (2009) 4787–4792.

[4] O. Abdelhafez, K.M. Amin, R.Z. Batran, T.J. Maher, S.A. Nada, S. Sethumadhavan, Synthesis, anticoagulant and PIVKA-II induced by new 4-hydroxycoumarin derivatives, Bioorg. Med. Chem. 18 (2010) 3371–3378.

[5] M. Mojzych, A. Dolashki, W. Voelter, Synthesis of pyrazolo[4,3-*e*][1,2,4]triazine sulfonamides, novel Sildenafil analogs with tyrosinase inhibitory activity, Bioorg. Med. Chem. 22 (2014) 6616–6624.

[6] P. Thanigaimalai, V.K. Sharma, K. Lee, C.Y. Yun, Y. Kim, S.H. Jung, Refinement of the pharmacophore of 3,4-dihydroquinazoline-2(1*H*)-thiones for their anti-melanogenesis activity, Bioorg. Med. Chem. 20 (2010) 4771–4773.

[7] P.G. Baraldi, M.G. Pavani, M.D.C. Nunez, P. Brigidi, B. Vitali, R. Gambari, R. Romagnoli, Antimicrobial and antitumor activity of *n*-heteroimmine-1,2,3-dithiazoles and their transformation in triazolo-, imidazo-, and pyrazolopirimidines, Bioorg. Med. Chem. Lett. 10 (2002) 449–456.

[8] A.H. Shamroukh, M.E.A. Zaki, E.M.H. Morsy, F.M. Abdel-Motti, F.M.E. Abdel-Megeid, Synthesis of pyrazolo[4',3':5,6]pyrano[2,3-*d*]pyrimidine derivatives for antiviral evaluation, Arch. Pharm. Chem. Life. Sci. 340 (2007) 236–243.

[9] P. Singh, M. Kaur, W. Holzer, Synthesis and evaluation of indole, pyrazole, chromone and pyrimidine based conjugates for tumor growth inhibitory activities–development of highly efficacious cytotoxic agents, Eur. J. Med. Chem. 45 (2010) 4968–4982.

[10] U. Yadava, M. Singh, M. Roychoudhury, Pyrazolo[3,4-*d*]pyrimidines as inhibitor of anti-coagulation and inflammation activities of phospholipase A_2: insight from molecular docking studies, J. Biol. Phys. 39 (2013) 419–438.

[11] R. Wang, W.M. Chai, Q. Yang, M.K. Wei, Y. Peng, 2-(4-Fluorophenyl)-quinazolin-4(3H)-one as a novel tyrosinase inhibitor: synthesis, inhibitory activity, and mechanism, Bioorg. Med. Chem. 24 (2016) 4620–4625.

[12] G. Zhang, Y. Zhangt, J. Yant, R. Chent, S. Wangt, Y. Mat, R. Wang, One-pot enantioselective synthesis of functionalized pyranocoumarins and 2-amino-4*H*-chromenes: discovery of a type of potent antibacterial agent, J. Org. Chem. 77 (2012) 878–888.

[13] J.N. Tan, H. Li, Y. Gu, Water mediated trapping of active methylene intermediates generated by IBX-induced oxidation of Baylis-Hillman adducts with nucleophiles, Green. Chem. 12 (2010) 1772–1782.

[14] N. Thomas, S.M. Zachariah, Pharmacological activities of chromene derivatives: an overview, Asian. J. Pharm. Clin. Res. 6 (2013) 11–15.

[15] O. Bruno, S. Schenone, A. Ranise, E. Barocelli, M. Chiavarini, V. Ballabeni, S. Bertoni, Synthesis and pharmacological screening of novel non-acidic gastroprotective antipyretic anti-inflammatory agents with anti-platelet properties. 5-alkyl/cycloalkylamino substituted 2-amino-5H-[1]benzopyrano[4,3-*d*] pyrimidines, Arzneim-Forsch 50 (2000) 140–147.

[16] N.R. Kamdar, D.D. Haveliwala, P.T. Mistry, S.K. Patel, Design, synthesis and *in vitro* evaluation of antitubercular and antimicrobial activity of some novel pyranopyrimidines, Eur. J. Med. Chem. 45 (2010) 5056–5063.

[17] X. Fan, D. Feng, Y. Qu, X. Zhang, J. Wang, P.M. Loiseau, G. Andrei, R. Snoeck, E.D. Clercq, Practical and efficient synthesis of pyrano[3,2-*c*]pyridone, pyrano[4,3-*b*]pyran and their hybrids with nucleoside as potential antiviral and antileishmanial agents, Bioorg. Med. Chem. 20 (2010) 809–813.

[18] M. Zayane, A. Rahmouni, M.D. Remadi, M.B. Mansour, A. Romdhane, H. Ben Jannet, Design and synthesis of antimicrobial, anticoagulant, and anticholinesterase hybrid molecules from 4-methylumbelliferone, J. Enzyme Inhib. Med. Chem. 31 (2016) 1566–1575.

[19] S.S. Kang, H.J. Kim, C. Jin, Y.S. Lee, Synthesis of tyrosinase inhibitory (4-oxo-4*H*-pyran-2-yl)acrylic acid ester derivatives, Bioorg. Med. Chem. 19 (2009) 188–191.

[20] O. Prakash, R. Kumar, R. Kumar, P. Tyagi, R.C. Kuhad, Organoiodine(III) mediated synthesis of 3,9-diaryl- and 3,9-difuryl-bis-1,2,4-triazolo[4,3-*a*][4,3-*c*]pyrimidines as antibacterial agents, Eur. J. Med. Chem. 42 (2007) 868–872.

[21] H.M. Ashour, M.G. Shaaban, O.H. Rizk, I.M. El-Ashmawy, Synthesis and biological evaluation of thieno [2′,3′:4,5]pyrimido[1,2-*b*][1,2,4]triazines and thieno[2,3-d][1,2,4]triazolo[1,5-*a*]pyrimidines as anti-inflammatory and analgesic agents, Eur. J. Med. Chem. 62 (2013) 341–351.

[22] Y. Wang, X. Sun, D. Yang, Z. Guo, X. Fan, M. Nie, F. Zhang, Y. Liu, Y. Li, Y. Wang, P. Gong, Y. Liu, Design, synthesis, and structure–activity relationship of novel and effective apixaban derivatives as FXa inhibitors containing 1,2,4-triazole/pyrrole derivatives as P2 binding element, Bioorg. Med. Chem. 24 (2016) 5646–5661.

[23] M. Rafiq, M. Saleem, M. Hanif, S.K. Kang, S.Y. Seo, K.H. Lee, Synthesis, structural elucidation and bioevaluation of 4-amino-1,2,4-3-thione's Schiff base dervatives, Arch. Pharm. Res. 39 (2016) 161–171.

[24] A. Romdhane, M.T. Martin, A. Ben Said, A. Jabrane, H. Ben Jannet, Synthesis of new naphto[2,1-*b*]pyrano[3,2-*e*][1,2,4]triazolo[*1,5-c*] pyrimidine derivatives and their evaluation as acetylcholinesterase inhibitors, J. Soc. Chim. Tun. 14 (2012) 127–131.

[25] A. Romdhane, J.-F. Gallard, M.A. Hamza, H. Ben Jannet, Synthesis of new phosphonate derivatives of naphtho[2,1-b[pyran]3,2-e][1,2,4]triazolo [1,5-c]pyrimidines, Phosphorus Sulfur Silicon 187 (2012) 612–618.

[26] A. Romdhane, H. Ben Jannet, Synthesis of new pyran and pyranoquinoline derivatives, Arab. J. Chem. 10 (2017) 3128–3134.

[27] M.N. Erichsen, T.H.V. Huynht, B. Abrahamsent, J.F. Bastlund, C. Bundgaard, O. Monrad, A. Bekker-Jensen, C.W. Nielsent, K. Fryden, A.A. Jensen, L. Bunch, Structure-activity relationship study of first selective inhibitor of excitatory amino

acid transporter subtype 1: 2-amino-4-(4-methoxyphenyl)-7-(naphthalen-1-yl)-5-oxo-5,6,7,8-tetrahydro-4H-chromene-3-carbonitrile (UCPH-101), J. Med. Chem. 53 (2010) 7180–7191.
[28] A. Rahmouni, S. Souiei, M.A. Belkacem, A. Romdhane, J. Bouajila, H. Ben Jannet, Synthesis and biological evaluation of novel pyrazolopyrimidines derivatives as anticancer and anti-5-lipoxygenase agents, Bioorg. Med. Chem. Lett. 66 (2016) 160–168.
[29] A. Rahmouni, A. Romdhane, M. Besbes, N. Elie, D. Touboul, H. Ben Jannet, Synthesis of novel pyrazolo[3,4-*d*]pyrimidinone derivatives as cytotoxic inhibitors, Med. J. Chem. 2 (2014) 679–690.
[30] A.M. Salahedine, A.M.F. Oliveira-Campos, L.M. Rodrigues, 3-Aminopyrroles and their application in the synthesis ofpyrrolo[3,2-*d*]pyrimidine (9-deazapurine) derivatives, ARKIVOC. XIV (2008) 180–190.
[31] H.A. Abdel-Aziz, N.A. Hamdy, A.M. Farag, I.M.I. Fakhr, Synthesis and reactions of 3-methylthiazolo[3,2-*a*]benzimidazole-2-carboxylic acid hydrazide: synthesis of some new pyrazole, 1,3-thiazoline, 1,2,4-triazole and 1,2,4-triazolo[3,4-*b*]-1,3,4-thiadiazine derivatives pendant to thiazolo[3,2-*a*]benzimidazole moiety, J. Chin. Chem. Soc. 54 (2007) 1573–1582.
[32] W.T. Ismaya, H.J. Rozeboom, A. Weijn, J.J. Mes, F. Fusetti, H.J. Wichers, B.W. Dijkstra, Crystal structure of agaricus bisporus mushroom tyrosinase: identity of the tetramer subunits and interaction with tropolone, Biochemistry 50 (2011) 5477–5487.
[33] M.B. Mansour, M. Dhahri, M. Hassine, N. Ajzenberg, L. Venisse, V. Ollivier, F. Chaubet, M. Jandrot-Perrus, R.M. Maaroufi, Highly sulfated dermatan sulfate from the skin of the ray *Raja montagui*: anticoagulant activity and mechanism of action, Comp. Biochem. Physiol. 156 (2010) 206–215.
[34] M. Gardelly, B. Trimech, M.A. Belkacem, M. Harbach, S. Abdelwahed, A. Mosbah, J. Bouajila, H. Ben Jannet, Synthesis of novel diazaphosphinanes coumarin derivatives with promoted cytotoxic and anti-tyrosinase activities, Bioorg. Med. Chem. 26 (2016) 2450–2454.
[35] Gaussian 09, M. J. Frisch, G. W. Trucks, H. B. Schlegel, G. E. Scuseria, M. A. Robb, J. R. Cheeseman, G. Scalmani, V. Barone, G. A. Petersson, H. Nakatsuji, X. Li, M. Caricato, A. Marenich, J. Bloino, B. G. Janesko, R. Gomperts, B. Mennucci, H. P. Hratchian, J. V. Ortiz, A. F. Izmaylov, J. L. Sonnenberg, D. Williams-Young, F. Ding, F. Lipparini, F. Egidi, J. Goings, B. Peng, A. Petrone, T. Henderson, D. Ranasinghe, V. G. Zakrzewski, J. Gao, N. Rega, G. Zheng, W. Liang, M. Hada, M. Ehara, K. Toyota, R. Fukuda, J. Hasegawa, M. Ishida, T. Nakajima, Y. Honda, O. Kitao, H. Nakai, T. Vreven, K. Throssell, J. A. Montgomery, Jr., J. E. Peralta, F. Ogliaro, M. Bearpark, J. J. Heyd, E. Brothers, K. N. Kudin, V. N. Staroverov, T. Keith, R. Kobayashi, J. Normand, K. Raghavachari, A. Rendell, J. C. Burant, S. S. Iyengar, J. Tomasi, M. Cossi, J. M. Millam, M. Klene, C. Adamo, R. Cammi, J. W. Ochterski, R. L. Martin, K. Morokuma, O. Farkas, J. B. Foresman, and D. J. Fox, Gaussian, Inc., Wallingford CT. 2010.
[36] http://autodock.scripps.edu/.
[37] The PyMOL Molecular Graphics System, Version 1.5.0.4 Schrö.